

Measurements and identifications of extreme ultraviolet spectra of highly-charged Sm and Er

Y.A. Podpaly, J.D. Gillaspy, J. Reader, Yu. Ralchenko

National Institute of Standards and Technology, Gaithersburg, MD 20899, USA

E-mail: yuri.podpaly@nist.gov

Abstract.

We report spectroscopic measurements of highly charged samarium and erbium performed at the National Institute of Standards and Technology (NIST) Electron Beam Ion Trap (EBIT). These measurements are in the extreme ultraviolet (EUV) range, and span electron beam energies from 0.98 keV to 3.00 keV. We observed 71 lines from Kr-like Sm^{26+} to Ni-like Sm^{34+} , connecting 83 energy levels, and 64 lines from Rb-like Er^{32+} to Ni-like Er^{40+} , connecting 78 energy levels. Of these lines, 64 in Sm and 60 in Er are new. Line identifications are performed using collisional-radiative modeling of the EBIT plasma. All spectral lines are assigned individual uncertainties, most in the ~ 0.001 nm range. Energy levels are derived from the wavelength measurements.

1. Introduction

Spectroscopy of rare earth elements has recently become a subject of active research due to the possible use of gadolinium and terbium as next generation light sources for extreme ultraviolet (EUV) lithography [1, 2]. There are also few available data about transitions of highly charged ions in the lanthanides, which makes this an important area for additional study.

In the NIST Atomic Spectra Database [3], erbium and samarium transitions are available primarily for Sm I and II and Er I, II, and III. Fewer data are available for more highly ionized ions. Some transitions have been measured on Electron Beam Ion Traps (EBITs) in the EUV and X-ray regimes [4, 5, 6, 7]. Much of the available data have been generated from laser produced plasmas [8, 9, 10, 11, 12, 13, 14, 15, 16]. Highly charged samarium has also been observed in tokamak plasmas [17, 18, 19]. In highly charged erbium, likewise, there are limited available data, including that generated by EBITs [4, 20, 21], laser plasmas [10, 11, 12, 22], and tokamaks [17, 18, 23].

In this paper, we report Er and Sm $n=4$ transitions in the EUV, continuing on our previous studies of Gd [1] and Dy [24]. A full list of identifications, wavelengths, and wavelength uncertainties is generated, and we calculate energy levels with uncertainties for these ions as well. The intent of this research is to expand the number of measured transitions among the rare earth elements near those of interest for EUV light sources and provide a systematic accounting of uncertainties for transitions and energy levels.

2. Experiment

This work was performed at the NIST EBIT [25]. Sm spectra were studied at twelve electron beam energies between 0.98 keV and 2.2 keV, and Er spectra were studied at twelve beam energies between 1.3 keV and 3.0 keV. These energies are sufficient to produce ions between approximately Rb-like and Ni-like ionization stages [3]. Beam currents varied between 15 mA and 86 mA. Plasma confinement was achieved, as usual, through the electrostatic trapping via the electron beam, two drift tubes (at 500 V and 220 V), and a 2.8 T axial magnetic field. Er and Sm were injected into the trap by using a multi-cathode Metal Vapor Vacuum Arc (MeVVA) [26]. The trap was emptied and new ions were injected from the MeVVA every 10 seconds.

Elements used for calibration were introduced by the MeVVA, by the gas injection system (described in [27]), or were present as intrinsic impurities.

Spectra were recorded with a spectrometer designed for use in the EUV [28]. The spectrometer is a flat-field variable-line spacing type grating spectrometer. Data were collected with a 2048 pixel \times 512 pixel (13.5 μm x 13.5 μm pixel dimensions) liquid-nitrogen-cooled charge coupled device (CCD). Spectra were taken as ten one-minute exposures, and a cosmic ray filtering program was used to automatically remove data that were outside of five Poisson standard deviations of the signal, effectively removing the majority of the cosmic rays and aberrant electronic noise. The spectral range for Sm measurements covered approximately 4 nm to 20 nm, and for Er approximately 3 nm to 17 nm.

Calibration of the samarium spectra was accomplished using twelve lines from Ne^{4+} through Ne^{7+} , one line of Fe^{23+} , one line of Fe^{22+} , and one line of Ba^{26+} . Spectra of neon were taken at 2 keV and 4 keV, iron was taken at 4 keV, and barium, which is an intrinsic impurity, was taken at 5.8 keV. Calibration of the erbium spectra was performed using twelve lines from Ne^{4+} through Ne^{7+} , four lines from Xe^{43+} and Xe^{42+} , one line from Ba^{45+} , one line from O^{4+} , and one line from O^{5+} . Spectra of neon were taken at 2 keV and 4 keV, xenon and barium at 5.8 keV, and oxygen at 1.8 keV. All lines were fit with unweighted Gaussian profiles, and uncertainties were generated for each calibration point. Third order calibration polynomials relating wavelength to detector channel number were calculated, and confidence intervals were generated from which calibration uncertainties were derived. By setting the requirement that the calibration polynomial fit had $\chi^2 \approx n - N$, where n is the number of calibration points and N is the degrees of freedom of the calibration curve [29], the systematic uncertainty was estimated. For samarium, the systematic uncertainty was found to be 0.00055 nm; for erbium, the systematic uncertainty was found to be 0.0010 nm.

Spectra were recorded at a variety of energies; typical results are shown in figures 1 and 2. The intensities of the experimental spectra are given in the analog-to-digital units (ADU) of the CCD. Lines were fit with unweighted Gaussians, and statistical, systematic, and calibration confidence interval uncertainties were added in quadrature for each line to generate a total uncertainty.

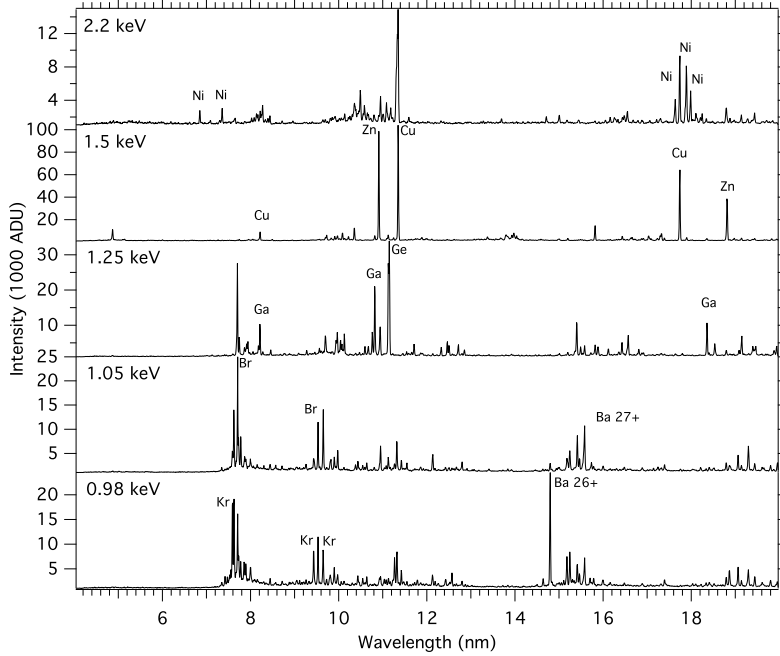


Figure 1. Samarium experimental results at five beam energies. Select lines are labeled by their isoelectronic sequence.

3. Collisional-Radiative Modeling

The measured spectra were analyzed with the collisional-radiative (CR) modeling that has been extensively described elsewhere (see, e.g., [30, 31, 32]), and therefore only the most relevant features will be described below. The line intensities for Er and Sm were calculated with the non-Maxwellian CR code NOMAD [33] utilizing atomic data generated with the Flexible Atomic Code (FAC) [34]. The level energies, radiative transition probabilities (allowed and forbidden), and electron-impact cross sections (excitation, deexcitation, ionization, and radiative recombination) were calculated for 8575 and 8570 levels in Sr-like to Ni-like ions of Er and Sm, respectively. The level energies were improved using an extended calculation taking into account all possible excitations within the $n=4$ complex, as described in [31]. The energies of the $3d^94l$ levels in Ni-like ions were taken from a more accurate relativistic many-body perturbation theory (RMBPT) calculation of [35]. The rate of charge exchange between highly-charged ions and neutral atoms in the trap was included

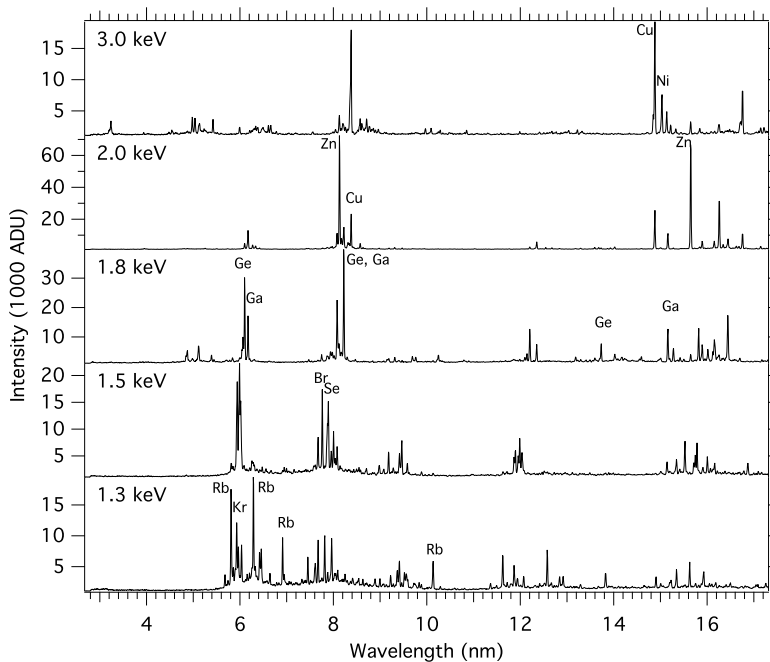


Figure 2. Erbium experimental results at five beam energies. Select lines are labeled by their isoelectronic sequence.

as the only free parameter, aside from a small shift in electron beam energy due to space charge as discussed below. A typical calculation of an EBIT spectrum would include 6-7 ionization stages since ions with ionization potentials larger than the beam energy are very weakly populated. The calculated bound-bound spectra were then Gaussian-broadened and convolved with the calculated efficiency curve of the EUV spectrometer.

Examples of agreement between theoretical and experimental spectra of Er are presented in figures 3 and 4. The agreement between theory and experiment for the Sm spectra is practically the same. The second order spectra are shown by the shifted dotted lines. Starting with figure 3, one can see that our CR modeling explains intensities and positions of all strong spectral lines. Note that the theoretical beam energy is lower than the nominal experimental energy; this is due to the space charge effects that are common in EBITs. Although for some lines there is a small shift in wavelength between theory and experiment, a very good match of line intensities allows us to unambiguously identify all prominent lines in the spectrum. For instance,

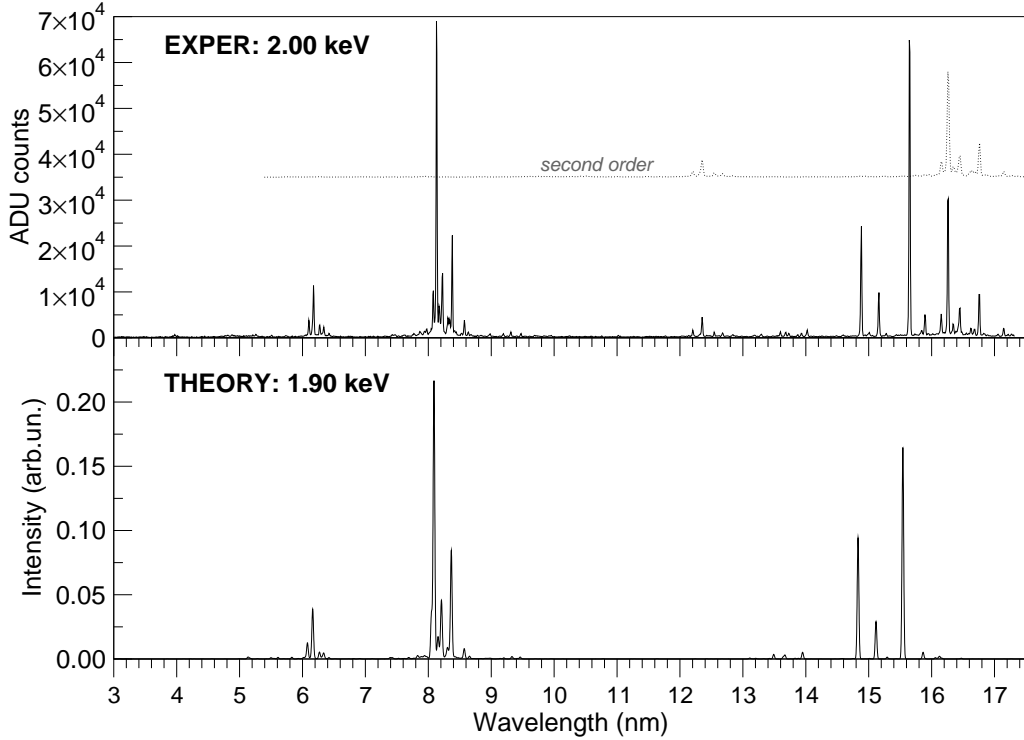


Figure 3. Comparison of the experimental spectrum of erbium with the theoretical spectrum.

the main groups of spectral lines near 8 nm and 15 nm are found to be due to the $4s_{1/2}-4p_{3/2}$ and $4s_{1/2}-4p_{1/2}$, respectively, in Cu-, Zn-, and Ga-like ions of Er.

The theoretical spectrum in Fig. 4 is also seen to agree well with the measured spectrum. The contributions from different ions are shown by different colors, while the total theoretical spectrum is marked by a black solid line. For this energy, the calculated ion populations are the following: [Kr]:[Br]:[As]:[Se]:[Ge] = 0.015:0.106:0.372:0.439:0.066 (see the inset in Fig. 4), and the remaining population (< 1%) is in the lower ions. Accordingly, the most prominent lines are due to transitions in As-like (blue) and Ge-like (orange) ions. Although a simple visual comparison allows us to identify practically all experimental lines, additional assistance in identification is provided by comparison of the intensity of the lines at the various beam energies. A similar E_{beam} -dependence of line intensities from a particular ionization stage is especially helpful in identification of blended lines.

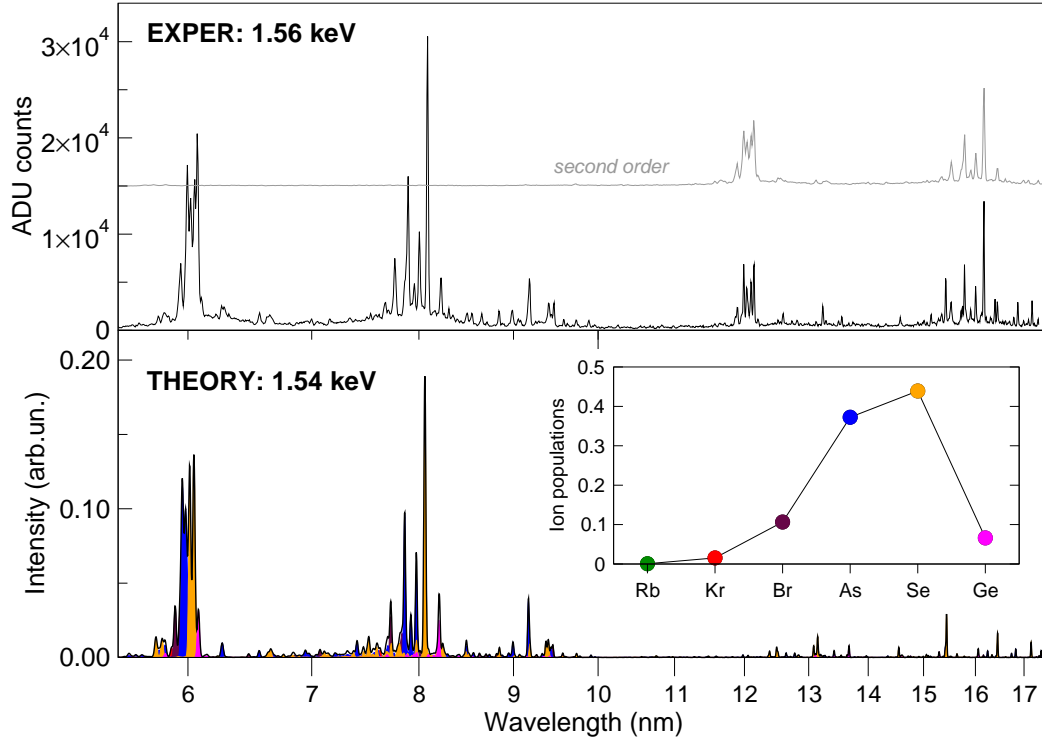


Figure 4. Comparison of the experimental spectrum of erbium with the theoretical spectrum. The inset shows the calculated ionization distribution at 1.54 keV. Contributions from different ionization stages are shown in different colors in the theoretical spectrum.

4. Results

Results of our measurements are shown in tables 1 and 2. Wavelengths calculated by FAC are presented as well. All uncertainties for wavelengths are reported as one standard deviation. The table also presents previous measurements of several spectral lines. If a line has significant blending with another line the letter ‘b’ is appended to the wavelength. For samarium, 71 lines were measured, with 64 of them new lines. For erbium, 64 lines were measured, with 60 of them new lines. In the erbium data, some of the Br-like lines were measured from their second orders and these wavelengths are marked with ‘(*2)’.

The level identifications are given in standard notations for relativistic configurations (e.g, $4p_+$ for $4p_{j=l+1/2}$ and $4d_-$ for $4d_{j=l-1/2}$). As is customary for

the FAC calculations, the electron pairs with total zero momentum are omitted. Since only the largest component of a wavefunction is presented, this may result in non-unique labels for some levels. For instance, levels 7 and 9 in As-like Sm are both shown in table 1 as belonging to the term $4d_-$ of configuration $4p^24d$. The calculations show that level 7 is composed of 45.7% of $4p^24d 4d_-$, 45.3% of $4s4p^4 (4s_+, (4p_+^2)_2)$, and 3.3% of $4s4p^4 ((4s_+, 4p_-)_1, (4p_+^3)_{3/2})$, while for level 9 the same relativistic terms have contributions of 49.9%, 34.2% and 5.3%, respectively. Such strong mixing is not uncommon in highly-charged N-shell ions.

The energy levels for samarium and erbium are reported in tables 3 and 4. The conversion factor from eV to cm^{-1} was $1 \text{ eV} = 8065.544219(18) \text{ cm}^{-1}$ [36]. The first energy level, ground level, is taken to have zero energy. In some cases, groups of levels are not connected to the ground level by measured radiative transitions, and therefore the energy of a reference level is taken from FAC or, in the case of Ni-like ions, from Ref. [35]. These levels are marked in our tables with the symbol $+$ followed by a letter. For those levels, the reported results are given as the weighted mean ($\propto 1/\sigma^2$) of the possible derivations. Since none of the derived levels have uncertainties less than 20 cm^{-1} , the results are all rounded to 10 cm^{-1} , unless they are from calculations.

For some lines, their identifications were validated by using the Ritz combination principle. For instance, the 8.2227 nm spectral line in Ga-like Er that corresponds to the transition between the ground state (level 1) and level 6, is blended by a strong line in the Ge-like ion, and therefore additional confirmation of its wavelength would be helpful. The ground state and the first excited level in this ion are both connected to levels 6 and 7, all four lines having been measured in the present experiment. The energy differences between the two lowest levels calculated from two pairs of measured wavelengths agree within approximately 0.1%, thereby confirming our identifications for all those lines, including the 1–6 transition. Similar analysis was performed for transitions in the Ni-like ions of Sm and Er.

For the spectral range analyzed here, there exist only a handful of other measurements for Sm and Er. Our wavelengths for Ni-like Sm agree very well with the low-resolution measurements from laser-produced plasmas [9]. The high-resolution measurements for Cu-like Sm and Er [10, 14] also agree with our results within experimental uncertainties. Similar level of agreement is observed for other measurements in Zn-like ions [11, 12]. This provides additional confidence in our measured wavelengths and identifications of spectral lines from other ions of Sm and

Er for which no measured lines are known.

For most cases, the FAC wavelengths deviate from the measured values to within a fraction of per cent. The only exception is the transitions in Ni-like Sm that connect level 35 with quantum numbers $3d^9 4d ((3d^3_{3/2}, 4d_-)_0)$ with levels 9 and 12. For this J=0 level the difference between theory and experiment reaches 1.6% for calculations that include double core excitations from n=3 into n=4 (value in table 3) and 4% for single 3–4 excitations. The RMBPT results of Ref. [35] do not contain J=0 levels and there is no other recent theoretical work addressing the energy of this particular level. We would like to point out that our measured 9–35 and 12–35 wavelengths can provide an interesting test for advanced atomic structure theories.

5. Conclusions

We report the results of EUV measurements of highly charged ions of samarium and erbium in an EBIT. One hundred and thirty-five lines are measured with individual uncertainties calculated for each line. From these transitions, a total of 161 energy levels were derived and uncertainties were assigned to each value. Overall, the agreement between theory and experiment is excellent with respect to the intensities of the lines and very good for the wavelengths. Our line identifications agree very well with the already known data for Ni-, Cu-, and Zn-like ions.

6. Acknowledgments

The authors would like to thank J. Smiga for assistance with calibration of the erbium spectra. This work was funded in part by the Office of Fusion Energy Sciences of the U.S. Department of Energy. Y.P. is supported by a postdoctoral appointment with the National Institute of Standards and Technology National Research Council Research Associateship Program.

References

- [1] Kilbane D, O’Sullivan G, Gillaspay J D, Ralchenko Yu, and Reader J 2012 *Phys. Rev. A* **86** 042503.
- [2] Churilov S S, Kildiyarova R R, Ryabtsev A N, and Sadovsky S V 2009 *Phys. Scr.* **80**(4) 045303.

- [3] Kramida A, Ralchenko Yu, Reader J, and NIST ASD Team 2013 NIST Atomic Spectra Database (ver. 5.1), [Online]. Available: <http://physics.nist.gov/asd>. National Institute of Standards and Technology, Gaithersburg, MD.
- [4] Gillaspay J D, Osin D, Ralchenko Yu, Reader J, and Blundell S A 2013 *Phys. Rev. A* **87** 062503.
- [5] Beiersdorfer P 1993 *AIP Conf. Proc.* **274**(1) 365.
- [6] Watanabe H, Currell F J, Fukami T, Kato D, Ohtani S, and Yamada C 2001 *Phys. Scr.* **T92** 122.
- [7] Watanabe H, Crosby D, Currell F J, Fukami T, Kato D, Ohtani S, *et al.* 2001 *Phys. Rev. A* **63** 042513.
- [8] Louzon D, Henis Z, Levi I, Hurvitz G, Ehrlich Y, Fraenkel M, Maman S, and Mandelbaum P 2009 *J. Opt. Soc. Am. B* **26**(5) 959–964.
- [9] Daido H, Ninomiya S, Takagi M, Kato Y, and Koike F 1999 *J. Opt. Soc. Am. B* **16**(2) 296.
- [10] Reader J and Luther G 1981 *Phys. Scr.* **24**(4) 732.
- [11] Reader J and Luther G 1980 *Phys. Rev. Lett.* **45** 609.
- [12] Acquista N and Reader J 1984 *J. Opt. Soc. Am. B* **1**(4) 649.
- [13] Ekberg J O, Feldman U, Seely J F, Brown C M, Reader J, and Acquista N 1987 *J. Opt. Soc. Am. B* **4**(12) 1913.
- [14] Doschek G A, Feldman U, Brown C M, Seely J F, Ekberg J O, Behring W E, and Richardson M C 1988 *J. Opt. Soc. Am. B* **5**(2) 243.
- [15] Ekberg J O, Feldman U, Hulburt E O, and Reader J 1988 *J. Opt. Soc. Am. B* **5**(6) 1275.
- [16] Wyart J F, Fajardo M, Miβualla T, Gauthier J C, Chenais-Popovics C, Klopfel D, *et al.* 1999 *Phys. Scr.* **T83** 35.
- [17] Sugar J, Kaufman V, and Rowan W L 1993 *J. Opt. Soc. Am. B* **10**(8) 1321.
- [18] Sugar J, Kaufman V, and Rowan W L 1993 *J. Opt. Soc. Am. B* **10**(5) 799.
- [19] Finkenthal M, Moos H W, Bar-Shalom A, Spector N, Zigler A, and Yarkoni E 1988 *Phys. Rev. A* **38**(1) 288.
- [20] Elliott S R, Beiersdorfer P, and Nilsen J 1995 *Phys. Rev. A* **51** 1683.
- [21] Elliott S R, Beiersdorfer P, MacGowan B J, and Nilsen J 1995 *Phys. Rev. A* **52** 2689.
- [22] Reader J 1983 *J. Opt. Soc. Am.* **73**(1) 63.
- [23] Sugar J, Kaufman V, and Rowan W L 1993 *J. Opt. Soc. Am. B* **10**(11) 1977.
- [24] Kilbane D, O’Sullivan G, Podpaly Y A, Gillaspay J D, Reader J, Ralchenko Yu 2014 *Eur. Phys J. D.* **68**(8) 222
- [25] Gillaspay J D, Roberts J R, Brown C M, and Feldman U 1997 *Phys. Scr.* **T71** 99.
- [26] Holland G E, Boyer C N, Seely J F, Tan J N, Pomeroy J D, and Gillaspay J D 2005 *Rev. Sci. Instrum.* **76** 073304.
- [27] Fahy K, Sokell E, O’Sullivan G, Aguilar A, Pomeroy J M, Tan J N, *et al.* 2007 *Phys. Rev. A* **75** 032520.
- [28] Blagojevic B, Le Bigot E O, Fahy K, Aguilar A, Makonyi K, Takacs E, *et al.* 2005 *Rev. Sci. Instrum.* **76**(8) 083102.
- [29] Hughes I and Hase T 2012 *Measurements and their Uncertainties* (Oxford University Press)
- [30] Ralchenko Yu, Draganić I N, Tan J N, Gillaspay J D, Pomeroy J M, Reader J, *et al.* 2008 *J. Phys. B*, **41** 021003.

- [31] Draganić I N, Ralchenko Yu, Reader J, Gillaspay J D, Tan J N, Pomeroy J M, Brewer S M, and Osin D 2011 *J. Phys. B*, 44:025001.
- [32] Ralchenko Yu, Draganić I N, Osin D, Gillaspay J D, and Reader J 2011 *Phys. Rev. A* **83** 032517.
- [33] Ralchenko Yu and Maron Y 2001 *J. Quant. Spectrosc. Ra.* **71**(2–6) 609.
- [34] Gu M F 2008 *Can. J. Phys.* **86** 675–689.
- [35] Safronova U I, Safronova A S, Hamasha S M, and Beiersdorfer P. 2006 *Atom. Data. Nucl. Data*, 92(1) 47.
- [36] Mohr P J, Taylor B N, and Newell D B 2012 *Rev. Mod. Phys.* **84** 1527

Table 1: Wavelengths (nm) of highly charged samarium. The numbers in parentheses are the wavelength uncertainties in units of the last significant digit. The numbers in square brackets in column “FAC” are the ordinal numbers for the lower and upper levels. b-blended line.

Stage	Lower Level		Upper Level		Wavelength	FAC	Prev. Exp.
	Conf.	State	Conf.	State			
34+ [Ni]	$3d^9 4p$	$((3d_-^3)_{3/2}, 4p_-)_1$	$3d^9 4d$	$((3d_-^3)_{3/2}, 4d_-)_0$	6.8494(7)	6.7384 [9-35]	6.85(2) ^a
34+ [Ni]	$3d^9 4p$	$((3d_+^5)_{5/2}, 4p_+)_1$	$3d^9 4d$	$((3d_-^3)_{3/2}, 4d_-)_0$	7.3563(8)	7.2344 [12-35]	7.36(2) ^a
34+ [Ni]	$3d^9 4p$	$((3d_+^5)_{5/2}, 4p_+)_4$	$3d^9 4d$	$((3d_+^5)_{5/2}, 4d_+)_5$	10.4908(11)	10.4800 [10-23]	
34+ [Ni]	$3d^9 4s$	$((3d_+^5)_{5/2}, 4s_+)_3$	$3d^9 4p$	$((3d_+^5)_{5/2}, 4p_-)_3$	17.6366(17)	17.5836 [2-7]	
34+ [Ni]	$3d^9 4s$	$((3d_+^5)_{5/2}, 4s_+)_3$	$3d^9 4p$	$((3d_+^5)_{5/2}, 4p_-)_2$	17.8926(14)	17.8722 [2-6]	
34+ [Ni]	$3d^9 4s$	$((3d_+^5)_{5/2}, 4s_+)_2$	$3d^9 4p$	$((3d_+^5)_{5/2}, 4p_-)_3$	17.9864(16)	17.9661 [3-7]	
34+ [Ni]	$3d^9 4s$	$((3d_-^3)_{3/2}, 4s_+)_2$	$3d^9 4p$	$((3d_-^3)_{3/2}, 4p_-)_2$	18.1084(20)	18.0985 [5-8]	
34+ [Ni]	$3d^9 4s$	$((3d_+^5)_{5/2}, 4s_+)_2$	$3d^9 4p$	$((3d_+^5)_{5/2}, 4p_-)_2$	18.2491(16)	18.2674 [3-6]	
33+ [Cu]	$4p$	$4p_-$	$4d$	$4d_-$	8.2176(7)b	8.2193 [2-4]	8.2206(15) ^b 8.2155(15) ^c
33+ [Cu]	$4d$	$4d_+$	$4f$	$4f_+$	10.2238(7)	10.2183 [5-7]	10.2249(15) ^b 10.2223(15) ^c
33+ [Cu]	$4p$	$4p_+$	$4d$	$4d_+$	10.3555(7)	10.3588 [3-5]	10.3571(15) ^b 10.3551(15) ^c
33+ [Cu]	$4s$	$4s_+$	$4p$	$4p_+$	11.3516(7)	11.1969 [1-3]	11.3509(15) ^b 11.3504(15) ^c
33+ [Cu]	$4s$	$4s_+$	$4p$	$4p_-$	17.7416(13)	17.3523 [1-2]	17.7450 ^d
32+ [Zn]	$4s4d$	$(4s_+, 4d_+)_2$	$4s4f$	$(4s_+, 4f_+)_3$	9.9127(7)	9.8855 [14-30]	
32+ [Zn]	$4s4p$	$(4s_+, 4p_+)_1$	$4s4d$	$(4s_+, 4d_+)_2$	10.0851(7)	10.0602 [5-14]	
32+ [Zn]	$4s^2$	$(4s_+^2)_0$	$4s4p$	$(4s_+, 4p_+)_1$	10.9125(6)	10.8361 [1-5]	10.911(2) ^e

32+ [Zn]	4s4p	(4s ₊ , 4p ₋) ₁	4p ²	(4p ₋ , 4p ₊) ₂	11.2465(8)	11.2393 [3-8]
32+ [Zn]	4s ²	(4s ₊ ²) ₀	4s4p	(4s ₊ , 4p ₋) ₁	18.8153(19)	18.658 [1-3]
31+ [Ga]	4p	4p ₋	4d	4d ₋	7.7461(8)	7.7150 [1-11]
31+ [Ga]	4p	4p ₋	4s4p ₂	(4s ₊ , (4p ₊ ²) ₂) _{3/2}	8.2146(7)	8.1951 [1-9]
31+ [Ga]	4p	4p ₊	4d	4d ₋	10.1294(7)	10.0619[2-11]
31+ [Ga]	4p	4p ₋	4s4p ²	(4s ₊ , (4p ₊ ²) ₂) _{5/2}	10.8203(7)	10.7701 [1-7]
31+ [Ga]	4p	4p ₊	4s4p ²	(4s ₊ , (4p ₊) ₂) _{3/2}	10.9448(20)b	10.8942 [2-9]
31+ [Ga]	4p	4p ₋	4s4p ²	((4s ₊ , 4p ₋) ₁ , 4p ₊) _{1/2}	11.1279(7)	11.1055 [1-6]
31+ [Ga]	4p	4p ₊	4s4p ²	((4s ₊ , 4p ₋) ₁ , 4p ₊) _{1/2}	16.8114(11)	16.7187 [2-6]
31+ [Ga]	4p	4p ₋	4s4p ²	4s ₊	18.3603(16)	18.3159 [1-3]
31+ [Ga]	4p	4p ₊	4s4p ²	((4s ₊ , 4p ₋) ₁ , 4p ₊) _{5/2}	19.1476(22)	19.1158 [2-5]
30+ [Ge]	4p ²	(4p ₋ ²) ₀	4p4d	(4p ₋ , 4d ₋) ₁	7.7020(7)	7.6492 [1-16]
30+ [Ge]	4p ²	(4p ₋ , 4p ₊) ₂	4p4d	(4p ₊ , 4d ₋) ₃	7.9406(7)	7.8988 [3-23]
30+ [Ge]	4p ²	(4p ₋ ²) ₀	4s4p ³	((4s ₊ , 4p ₋) ₁ , (4p ₊ ²) ₀) ₁	8.1809(10)	8.135 [1-13]
30+ [Ge]	4p ²	(4p ₋ , 4p ₊) ₁	4p4d	(4p ₋ , 4d ₋) ₁	9.6994(7)b	9.6032 [2-16]
30+ [Ge]	4p ²	(4p ₋ , 4p ₊) ₂	4p4d	(4p ₋ , 4d ₊) ₃	9.9701(7)	9.9429 [3-15]
30+ [Ge]	4s4p ³	(4s ₊ , 4p ₊) ₁	4s4p ² 4d	(4s ₊ , 4d ₊) ₂	10.0424(7)	10.0244 [7-33]
30+ [Ge]	4p ²	(4p ₋ , 4p ₊) ₂	4s4d	(4p ₋ , 4d ₋) ₂	10.6728(9)	10.6342 [3-14]
30+ [Ge]	4p ²	(4p ₋ , 4p ₊) ₂	4s4p ³	((4s ₊ , 4p ₋) ₁ , (4p ₊ ²) ₀) ₁	10.7648(8)	10.6784 [3-13]
30+ [Ge]	4p ²	(4p ₋ , 4p ₊) ₁	4p4p ³	((4s ₊ , 4p ₋) ₁ , (4p ₊ ²) ₂) ₁	10.9423(7)b	10.8984 [2-12]
30+ [Ge]	4p ²	(4p ₋ ²) ₀	4s4p ³	(4s ₊ , 4p ₊) ₁	11.1501(7)	11.1261 [1-7]
30+ [Ge]	4p ²	(4p ₋ , 4p ₊) ₂	4p4d	(4p ₋ , 4d ₋) ₂	11.7114(8)	11.7236 [3-10]
30+ [Ge]	4p ²	(4p ₋ , 4p ₊) ₂	4s4p ³	((4s ₊ , 4p ₋) ₁ , (4p ₊ ²) ₂) ₃	12.3270(11)	12.3630 [3-9]
30+ [Ge]	4p ²	(4p ₋ , 4p ₊) ₂	4s4p ³	(4s ₊ , 4p ₊) ₁	16.5715(9)	16.5015 [3-7]
29+ [As]	4p ³	4p ₊	4p ² 4d	((4p ₋ , 4p ₊) ₂ , 4d ₋) _{1/2}	7.6812(7)b	7.6310 [1-24]
29+ [As]	4p ³	4p ₊	4p ² 4d	((4p ₋ , 4p ₊) ₂ , 4d ₊) _{5/2}	7.6812(7)b	7.6372 [1-23]

29+	[As]	$4p^3$	$4p_+$	$4p^24d$	$((4p_-, 4p_+)_2, 4d_-)_{3/2}$	7.8640(8)	7.8150 [1-22]
29+	[As]	$4p^3$	$4p_+$	$4p^24d$	$((4p_-, 4p_+)_1, 4d_+)_{5/2}$	7.9127(8)	7.8810 [1-21]
29+	[As]	$4p^3$	$(4p_-, (4p_+^2)_2)_{3/2}$	$4p^24d$	$((4p_-, 4p_+)_2, 4d_+)_{5/2}$	9.0907(8)	8.9946 [2-28]
29+	[As]	$4p^3$	$4p_+$	$4p^24d$	$4d_+$	9.9388(8)	9.9104[1-10]
29+	[As]	$4p^3$	$4p_+$	$4p^24d$	$4d_-$	10.5983(7)	10.5592[1-9]
29+	[As]	$4p^3$	$4p_+$	$4p^24d$	$4d_-$	11.5407(7)	11.5409[1-7]
29+	[As]	$4p^3$	$4p_+$	$4s4p^4$	$(4s_+, (4p_+^2)_2)_{5/2}$	12.5081(7)	12.5409 [1-6]
29+	[As]	$4p^3$	$(4p_-, (4p_+^2)_2)_{5/2}$	$4p^24d$	$4d_-$	17.3265(12)	17.3085 [3-7]
29+	[As]	$4p^3$	$(4p_-, (4p_+^2)_0)_{1/2}$	$4s4p^4$	$(4s_+, (4p_+^2)_0)_{1/2}$	17.6760(14)	17.6538 [4-8]
29+	[As]	$4p^3$	$(4p_-, (4p_+^2)_2)_{3/2}$	$4s4p^4$	$(4s_+, (4p_+^2)_2)_{5/2}$	18.4066(17)	18.4182 [2-6]
29+	[As]	$4p^3$	$(4p_-, (4p_+^2)_2)_{5/2}$	$4s4p^4$	$(4s_+, (4p_+^2)_2)_{5/2}$	19.6006(24)	19.6597 [3-6]
28+	[Se]	$4p^4$	$(4p_+^2)_2$	$4p^34d$	$((4p_-, (4p_+^2)_2)_{3/2}, 4d_-)_3$	7.7090(7)	7.6446 [1-32]
28+	[Se]	$4p^4$	$(4p_+^2)_2$	$4p^34d$	$((4p_-, (4p_+^2)_2)_{5/2}, 4d_-)_2$	7.7800(7)	7.7198 [1-29]
28+	[Se]	$4p^4$	$(4p_+^2)_2$	$4p^34d$	$(4p_+, 4d_+)_3$	9.6502(7)b	9.6084 [1-14]
28+	[Se]	$4p^4$	$(4p_+^2)_0$	$4p^34d$	$(4p_+, 4d_+)_1$	9.8209(13)	9.7842 [2-15]
28+	[Se]	$4p^4$	$(4p_+^2)_2$	$4p^34d$	$(4p_+, 4d_+)_2$	9.9790(8)	9.9450 [1-13]
28+	[Se]	$4p^34d$	$((4p_+^3)_{3/2}, 4d_+)_4$	$4s4p^44d$	$((4s_+, (4p_+^2)_0)_{1/2}, 4d_+)_3$	10.4393(7)	10.4893 [12-65]
28+	[Se]	$4p^4$	$(4p_+^2)_2$	$4p^34d$	$(4p_+, 4d_-)_3$	10.9516(9)	10.9310 [1-10]
28+	[Se]	$4p^4$	$(4p_+^2)_2$	$4p^34d$	$(4p_+, 4d_-)_1$	11.5467(11)	11.5440 [1-7]
28+	[Se]	$4p^4$	$(4p_+^2)_2$	$4s4p^5$	$(4s_+, (4p_+)_{3/2})_2$	12.1372(8)	12.1546 [1-6]
27+	[Br]	$4p^5$	$(4p_+^3)_{3/2}$	$4p^44d$	$((4p_-, (4p_+^3)_{3/2})_2, 4d_-)_{5/2}$	7.6242(7)	7.5549 [1-27]
27+	[Br]	$4p^5$	$(4p_+^3)_{3/2}$	$4p^44d$	$(4p_-, (4p_+^3)_2, 4d_-)_{1/2}$	7.7321(12)	7.6606 [1-25]
27+	[Br]	$4p^5$	$(4p_+^3)_{3/2}$	$4p^44d$	$((4p_+^2)_2, 4d_{+5/2})_{5/2}$	9.5321(7)	9.4986 [1-14]
27+	[Br]	$4p^5$	$(4p_+^3)_{3/2}$	$4s$	$4s_+$	9.6479(7)b	9.6142 [1-13]
27+	[Br]	$4p^5$	$(4p_+^3)_{3/2}$	$4p^44d$	$((4p_+^2)_0, 4d_{+5/2})_{5/2}$	9.8126(9)	9.7848 [1-12]
27+	[Br]	$4p^5$	$(4p_+^3)_{3/2}$	$4p^44d$	$((4p_+^2)_2, 4d_{+5/2})_{1/2}$	9.9000(7)	9.8682 [1-11]
26+	[Kr]	$4p^6$	$(4p_+^4)_0$	$4p^54d$	$(4p_-, 4d_-)_1$	7.5901(7)	7.4940 [1-13]

26+ [Kr]	$4p^6$	$(4p_+^4)_0$	$4p^5 4d$	$((4p_+^3)_{3/2}, 4d_+)_1$	9.4330(7)	9.3654 [1-9]
26+ [Kr]	$4p^6$	$(4p_+^4)_0$	$4p^5 4d$	$((4p_+^3)_{3/2}, 4d_-)_1$	11.2694(9)	11.2303 [1-3]
<hr/>						
$a - [9], b - [10], c - [14], d - [19], e - [11], f - [12]$						

Table 2: Wavelengths (nm) of highly charged erbium. The numbers in parentheses are the wavelength uncertainties in units of the last significant digit. The numbers in square brackets in column “FAC” are the ordinal numbers for the lower and upper levels. b-blended line. (*2)-wavelength derived from second order measurement.

Stage	Lower Level		Upper Level		Wavelength	FAC	Prev. Exp.
	Conf.	State	Conf.	State			
40+ [Ni]	$3d^9 4p$	$((3d_+^5)_{5/2}, 4p_+)_4$	$3d^9 4d$	$((3d_+^5)_{5/2}, 4d_+)_5$	8.7119(12)	8.7307 [10-23]	
40+ [Ni]	$3d^9 4s$	$((3d_+^5)_{5/2}, 4s_+)_3$	$3d^9 4p$	$((3d_+^5)_{5/2}, 4p_-)_3$	14.8490(14)	14.8038 [2-7]	
40+ [Ni]	$3d^9 4s$	$((3d_+^5)_{5/2}, 4s_+)_3$	$3d^9 4p$	$((3d_+^5)_{5/2}, 4p_-)_2$	15.0340(12)	15.0153 [2-6]	
40+ [Ni]	$3d^9 4s$	$((3d_+^5)_{5/2}, 4s_+)_2$	$3d^9 4p$	$((3d_+^5)_{5/2}, 4p_-)_3$	15.1355(13)	15.1163 [3-7]	
40+ [Ni]	$3d^9 4s$	$((3d_+^3)_{3/2}, 4s_+)_2$	$3d^9 4p$	$((3d_+^3)_{3/2}, 4p_-)_2$	15.2200(12)	15.2079 [5-8]	
40+ [Ni]	$3d^9 4s$	$((3d_+^5)_{5/2}, 4s_+)_2$	$3d^9 4p$	$((3d_+^5)_{5/2}, 4p_-)_2$	15.3297(12)	15.3369 [3-6]	
39+ [Cu]	$4p$	$4p_-$	$4d$	$4d_-$	6.3391(14)	6.3379 [2-4]	6.3403(15) ^a
39+ [Cu]	$4s$	$4s_+$	$4p$	$4p_+$	8.3796(12)	8.3654 [1-3]	8.3813(15) ^a
39+ [Cu]	$4p$	$4p_+$	$4d$	$4d_+$	8.5733(12)	8.5712 [3-5]	8.5760(15) ^a
39+ [Cu]	$4s$	$4s_+$	$4p$	$4p_-$	14.8817(13)	14.8305 [1-2]	
38+ [Zn]	$4s4p$	$(4s_+, 4p_-)_1$	$4s4d$	$(4s_+, 4d_-)_2$	6.2733(12)	6.2686 [3-10]	
38+ [Zn]	$4s^2$	$(4s_+^2)_0$	$4s4p$	$(4s_+, 4p_+)_1$	8.1312(12)	8.0900 [1-5]	8.131(2) ^b
38+ [Zn]	$4s4p$	$(4s_+, 4p_+)_1$	$4s4d$	$(4s_+, 4d_+)_2$	8.1732(21)	8.1548 [5-14]	
38+ [Zn]	$4s^2$	$(4s_+^2)_0$	$4s4p$	$(4s_+, 4p_-)_1$	15.6499(12)	15.5430 [1-3]	
37+ [Ga]	$4p$	$4p_-$	$4d$	$4d_-$	6.1755(12)	6.1626 [1-9]	
37+ [Ga]	$4p$	$4p_-$	$4s4p^2$	$((4s_+, 4p_-)_1, 4p_+)_1/2$	8.0777(14)	8.0497 [1-7]	
37+ [Ga]	$4p$	$4p_-$	$4s4p^2$	$((4s_+, 4p_-)_1, 4p_+)_3/2$	8.2227(12)b	8.2109 [1-6]	
37+ [Ga]	$4p$	$4p_-$	$4s4p^2$	$((4s_+, 4p_-)_0, 4p_+)_3/2$	9.3102(12)	9.3281 [1-4]	
37+ [Ga]	$4p$	$4p_+$	$4s4p^2$	$((4s_+, 4p_-)_2, 4p_+)_1/2$	13.5942(13)	13.4904 [2-7]	

37+ [Ga]	4p	4p ₊	4s4p ²	((4s ₊ , 4p ₋) ₁ , 4p ₊) _{3/2}	14.0226(13)	13.9493 [2-6]
37+ [Ga]	4p	4p ₋	4s4p ²	4s ₊	15.1604(12)	15.1163 [1-3]
37+ [Ga]	4p	4p ₊	4s4p ²	((4s ₊ , 4p ₋) ₁ , 4p ₊) _{5/2}	15.8957(13)	15.8643 [2-5]
36+ [Ge]	4p ²	(4p ₋ ²) ₀	4p4d	(4p ₋ , 4d ₋) ₁	6.1041(12)	6.0786 [1-11]
36+ [Ge]	4p ²	(4p ₋ ²) ₀	4s4p ³	(4s ₊ , 4p ₊) ₁	8.2214(12)b	8.2014 [1-7]
36+ [Ge]	4p ²	(4p ₋ , 4p ₊) ₂	4s4p ³	(4s ₊ , 4p ₊) ₁	13.7334(12)	13.6693 [3-7]
35+ [As]	4p ³	4p ₊	4p ² 4d	((4p ₋ , 4p ₊) ₂ , 4d ₋) _{3/2}	6.0497(13)	6.0137 [1-21]
35+ [As]	4p ³	4p ₊	4p ² 4d	((4p ₋ , 4p ₊) ₁ , 4d ₋) _{5/2}	6.0727(23)	6.0435 [1-20]
35+ [As]	4p ³	(4p ₋ , (4p ₊) ₀) _{1/2}	4p ² 4d	((4p ₋ , 4p ₊) ₁ , 4d ₊) _{7/2}	8.8392(13)	8.8433 [3-17]
35+ [As]	4p ³	(4p ₋ , (4p ₊ ²) ₂) _{3/2}	4s4p ⁴	(4s ₊ , (4p ₊ ²) ₂) _{5/2}	15.4209(13)	15.4358 [2-7]
35+ [As]	4p ³	(4p ₋ , (4p ₊ ²) ₂) _{5/2}	4s4p ⁴	(4s ₊ , (4p ₊ ²) ₂) _{5/2}	16.3966(13)	16.4483 [3-7]
35+ [As]	4p ³	(4p ₋ , (4p ₊ ²) ₂) _{5/2}	4p ² 4d	4d ₋	17.1697(15)	17.1498 [3-6]
34+ [Se]	4p ⁴	(4p ₊ ²) ₂	4p ³ 4d	((4p ₋ , (4p ₊ ²) ₂) _{3/2} , 4d ₋) ₃	5.9929(18)	5.9580 [1-30]
34+ [Se]	4p ⁴	(4p ₊ ²) ₂	4p ³ 4d	((4p ₋ , (4p ₊ ²) ₂) _{5/2} , 4d ₋) ₂	6.0230(22)	5.9797 [1-29]
34+ [Se]	4p ⁴	(4p ₊ ²) ₂	4p ³ 4d	(4p ₊ , 4d ₊) ₃	7.8933(12)	7.8593 [1-14]
34+ [Se]	4p ⁴	(4p ₊ ²) ₀	4p ³ 4d	(4p ₊ , 4d ₊) ₁	7.9546(12)	7.9199 [2-15]
34+ [Se]	4p ⁴	(4p ₊ ²) ₂	4p ³ 4d	(4p ₊ , 4d ₊) ₂	8.0042(12)	7.9737 [1-13]
34+ [Se]	4p ⁴	(4p ₊ ²) ₂	4p ³ 4d	(4p ₊ , 4d ₋) ₃	9.1787(15)	9.169 [1-9]
33+ [Br]	4p ⁵	(4p ₊ ³) _{3/2}	4p ⁴ 4d	((4p ₋ , (4p ₊ ³) _{3/2}) ₂ , 4d ₋) _{5/2}	5.9479(6)(*2)	5.9049 [1-26]
33+ [Br]	4p ⁵	(4p ₊ ³) _{3/2}	4p ⁴ 4d	((4p ₋ , (4p ₊ ³) _{3/2}) ₂ , 4d ₋) _{3/2}	5.9789(7)b(*2)	5.9390 [1-25]
33+ [Br]	4p ⁵	(4p ₊ ³) _{3/2}	4p ⁴ 4d	((4p ₋ , (4p ₊ ³) _{3/2}) ₂ , 4d ₋) _{1/2}	5.9789(7)b(*2)	5.9443 [1-24]
33+ [Br]	4p ⁵	(4p ₊ ³) _{3/2}	4p ⁴ 4d	((4p ₊ ²) ₂ , 4d ₊) _{5/2}	7.7630(12)	7.7217 [1-14]
33+ [Br]	4p ⁵	(4p ₊ ³) _{3/2}	4s	4s ₊	7.8578(10)	7.8181[1-13]
33+ [Br]	4p ⁵	(4p ₊ ³) _{3/2}	4p ⁴ 4d	((4p ₊ ²) ₂ , 4d ₊) _{3/2}	7.8717(13)	7.8352 [1-12]
33+ [Br]	4p ⁵	(4p ₊ ³) _{3/2}	4p ⁴ 4d	((4p ₊ ²) ₂ , 4d ₊) _{1/2}	9.2830(14)	9.2630 [1-6]
33+ [Br]	4p ⁵	(4p ₊ ³) _{3/2}	4p ⁴ 4d	((4p ₊ ²) ₂ , 4d ₋) _{5/2}	9.4626(47)	9.4519 [1-5]

33+ [Br]	$4p^5$	$(4p_+^3)_{3/2}$	$4p^4 4d$	$((4p_+^2)_2, 4d_-)_{3/2}$	9.5823(12)	9.5710 [1-3]
32+ [Kr]	$4p^6$	$(4p_+^4)_0$	$4p^5 4d$	$(4p_-, 4d_-)_1$	5.9356(13)	5.8792 [1-13]
32+ [Kr]	$4p^6$	$(4p_+^4)_0$	$4p^5 4d$	$((4p_+^3)_{3/2}, 4d_+)_1$	7.6746(12)	7.6221 [1-9]
32+ [Kr]	$4p^6$	$(4p_+^4)_0$	$4p^5 4d$	$((4p_+^3)_{3/2}, 4d_-)_1$	9.4129(12)	9.3900 [1-3]
31+ [Rb]	$4d$	$4d_-$	$4p^5 4d^2$	$(4p_-, (4d_-^2)_2)_{3/2}$	5.8139(13)	5.7583 [1-45]
31+ [Rb]	$4d$	$4d_-$	$4p^5 4d^2$	$(4p_-, (4d_-^2)_0)_{1/2}$	5.9709(18)	5.9212 [1-40]
31+ [Rb]	$4d$	$4d_-$	$4p^5 4d^2$	$(4p_-, (4d_-^2)_2)_{5/2}$	6.2905(12)	6.2377 [1-34]
31+ [Rb]	$4d$	$4d_-$	$4f$	$4f_-$	6.9150(11)	6.8765[1-32]
31+ [Rb]	$4d$	$4d_-$	$4p^5 4d^2$	$((4p_+^3)_{3/2}, 4d_-)_3, 4d_+)_1/2$	7.4543(12)	7.3946 [1-28]
31+ [Rb]	$4d$	$4d_-$	$4p^5 4d^2$	$((4p_+^3)_{3/2}, 4d_-)_3, 4d_+)_3/2$	7.8144(12)	7.7673 [1-25]
31+ [Rb]	$4d$	$4d_-$	$4p^5 4d^2$	$((4p_+^3)_{3/2}, (4d_+^2)_4)_{5/2}$	7.9633(13) ^b	7.9128 [1-21]
31+ [Rb]	$4d$	$4d_-$	$4p^5 4d^2$	$((4p_+^3)_{3/2}, (4d_+^2)_2)_{5/2}$	7.9633(13) ^b	7.9255 [1-22]
31+ [Rb]	$4d$	$4d_-$	$4p^5 4d^2$	$((4p_+^3)_{3/2}, 4d_-)_3, 4d_+)_5/2$	8.2514(12)	8.2165 [1-17]
31+ [Rb]	$4d$	$4d_-$	$4p^5 4d^2$	$((4p_+^3)_{3/2}, 4d_-)_1, 4d_+)_3/2$	8.6289(12)	8.6045 [1-11]
31+ [Rb]	$4d$	$4d_-$	$4p^5 4d^2$	$((4p_+^3)_{3/2}, (4d_-^2)_0)_{3/2}$	8.8905(13)	8.8592 [1-8]
31+ [Rb]	$4d$	$4d_+$	$4p^5 4d^2$	$((4p_+^3)_{3/2}, 4d_-)_2, 4d_+)_7/2$	8.9963(12)	8.9544 [2-16]
31+ [Rb]	$4d$	$4d_+$	$4p^5 4d^2$	$((4p_+^3)_{3/2}, 4d_-)_3, 4d_+)_7/2$	9.2249(12)	9.1879 [2-14]
31+ [Rb]	$4d$	$4d_-$	$4p^5 4d^2$	$((4p_+^3)_{3/2}, (4d_-^2)_2)_{5/2}$	9.3670(13)	9.3340 [1-5]
31+ [Rb]	$4d$	$4d_+$	$4p^5 4d^2$	$((4p_+^3)_{3/2}, (4d_-^2)_2)_{7/2}$	10.1342(12)	10.0913 [2-6]

^a - [10], ^b - [12],

Table 3: Energy levels of highly charged samarium. RMBPT -relativistic many body perturbation theory [35], FAC - flexible atomic code [34], †-weighted average from two transitions, ††-weighted average from three transitions

Stage and sequence	Configuration	State	Level number (FAC)	Energy (cm ⁻¹)	Unc. (cm ⁻¹)
34+ [Ni]	3d ¹⁰	(3d ₊ ⁶) ₀	1	0	0
34+ [Ni]	3d ⁹ 4s	((3d ₊ ⁵) _{5/2} , 4s ₊) ₃	2	7 522 190	+x RMBPT
34+ [Ni]	3d ⁹ 4s	((3d ₊ ⁵) _{5/2} , 4s ₊) ₂	3	7 533 150	+x 50†
34+ [Ni]	3d ⁹ 4s	((3d ₋ ³) _{3/2} , 4s ₊) ₂	5	7 752 539	+y RMBPT
34+ [Ni]	3d ⁹ 4p	((3d ₊ ⁵) _{5/2} , 4p ₋) ₂	6	8 081 080	+x 40
34+ [Ni]	3d ⁹ 4p	((3d ₊ ⁵) _{5/2} , 4p ₋) ₃	7	8 089 190	+x 50
34+ [Ni]	3d ⁹ 4p	((3d ₋ ³) _{3/2} , 4p ₋) ₂	8	8 304 770	+y 60
34+ [Ni]	3d ⁹ 4p	((3d ₋ ³) _{3/2} , 4p ₋) ₁	9	8 322 930	+z RMBPT
34+ [Ni]	3d ⁹ 4p	((3d ₊ ⁵) _{5/2} , 4p ₊) ₄	10	8 404 586	+a FAC
34+ [Ni]	3d ⁹ 4p	((3d ₊ ⁵) _{5/2} , 4p ₊) ₁	12	8 423 520	+z 200
34+ [Ni]	3d ⁹ 4d	((3d ₊ ⁵) _{5/2} , 4d ₊) ₅	23	9 357 800	+a 100
34+ [Ni]	3d ⁹ 4d	((3d ₋ ³) _{3/2} , 4d ₋) ₀	35	9 782 910	+z 150
33+ [Cu]	4s	4s ₊	1	0	0
33+ [Cu]	4p	4p ₋	2	563 650	40
33+ [Cu]	4p	4p ₊	3	880 940	50
33+ [Cu]	4d	4d ₋	4	1 780 550	110
33+ [Cu]	4d	4d ₊	5	1 846 610	80
33+ [Cu]	4f	4f ₊	7	2 824 720	110
32+ [Zn]	4s ²	(4s ₊ ²) ₀	1	0	0
32+ [Zn]	4s4p	(4s ₊ , 4p ₋) ₁	3	531 480	50
32+ [Zn]	4s4p	(4s ₊ , 4p ₊) ₁	5	916 380	50

32+	[Zn]	$4p^2$	$(4p_-, 4p_-)_2$	8	1 420 650	80
32+	[Zn]	$4s4d$	$(4s_+, 4d_+)_2$	14	1 907 940	90
32+	[Zn]	$4s4f$	$(4s_+, 4f_+)_3$	30	2 916 740	110
31+	[Ga]	$4p$	$4p_-$	1	0	0
31+	[Ga]	$4p$	$4p_+$	2	303 790	50††
31+	[Ga]	$4s4p^2$	$4s_+$	3	544 650	50
31+	[Ga]	$4s4p^2$	$((4s_+, 4p_-)_1, 4p_+)_{5/2}$	5	826 040	80
31+	[Ga]	$4s4p^2$	$((4s_+, 4p_-)_1, 4p_+)_{3/2}$	6	898 640	50
31+	[Ga]	$4s4p^2$	$((4s_+, 4p_-)_1, 4p_+)_{1/2}$	7	924 190	60
31+	[Ga]	$4s4p^2$	$(4s_+, (4p_+^2)_2)_{3/2}$	9	1 217 350	100
31+	[Ga]	$4d$	$4d_-$	11	1 290 970	130
30+	[Ge]	$4p^2$	$(4p_-^2)_0$	1	0	0
30+	[Ge]	$4p^2$	$(4p_-, 4p_+)_1$	2	267 370	140
30+	[Ge]	$4p^2$	$(4p_-, 4p_+)_2$	3	293 400	60†
30+	[Ge]	$4s4p^3$	$(4s_+, 4p_+)_1$	7	896 850	50
30+	[Ge]	$4s4p^3$	$((4s_+, 4p_-)_1, (4p_+^2)_2)_3$	9	1 104 630	90
30+	[Ge]	$4p4d$	$(4p_-, 4d_-)_2$	10	1 147 270	80
30+	[Ge]	$4p4p^3$	$((4s_+, 4p_-)_1, (4p_+^2)_2)_1$	12	1 181 260	160
30+	[Ge]	$4s4p^3$	$((4s_+, 4p_-)_1, (4p_+^2)_0)_1$	13	1 222 350	160
30+	[Ge]	$4p4d$	$(4p_-, 4d_+)_2$	14	1 230 370	100
30+	[Ge]	$4p4d$	$(4p_-, 4d_+)_3$	15	1 296 400	90
30+	[Ge]	$4p4d$	$(4p_-, 4d_-)_1$	16	1 298 360	120
30+	[Ge]	$4p4d$	$(4p_+, 4d_-)_3$	23	1 552 740	130
30+	[Ge]	$4s4p^24d$	$(4s_+, 4d_+)_2$	33	1 892 630	900
29+	[As]	$4p^3$	$(4p_+^3)_{3/2}$	1	0	0
29+	[As]	$4p^3$	$(4p_-, (4p_+^2)_2)_{3/2}$	2	256 210	70
29+	[As]	$4p^3$	$(4p_-, (4p_+^2)_2)_{5/2}$	3	289 330	50†

29+	[As]	$4p^3$	$(4p_-, (4p_+^2)_0)_{1/2}$	4	331 860	+x	FAC
29+	[As]	$4s4p^4$	$(4s_+, (4p_+^2)_2)_{5/2}$	6	799 490		50
29+	[As]	$4p^24d$	$4d_-$	7	866 500		50
29+	[As]	$4s4p^3$	$(4s_+, (4p_+^2)_0)_{1/2}$	8	897 600	+x	50
29+	[As]	$4p^24d$	$4d_-$	9	943 540		60
29+	[As]	$4p^24d$	$4d_+$	10	1 006 160		100
29+	[As]	$4p^24d$	$((4p_-, 4p_+)_1, 4d_+)_{5/2}$	21	1 263 780		120
29+	[As]	$4p^24d$	$((4p_-, 4p_+)_2, 4d_-)_{3/2}$	22	1 271 620		120
29+	[As]	$4p^24d$	$((4p_-, 4p_+)_2, 4d_+)_{5/2}$	23	1 301 880b		120
29+	[As]	$4p^24d$	$((4p_-, 4p_+)_2, 4d_-)_{1/2}$	24	1 301 880b		120
29+	[As]	$4p^24d$	$((4p_-, (4p_+)_2), 4d_+)_{5/2}$	28	1 356 240		120
28+	[Se]	$4p^4$	$(4p_+^2)_2$	1	0		0
28+	[Se]	$4p^4$	$(4p_+^2)_0$	2	53 669	+x	FAC
28+	[Se]	$4s4p^5$	$(4s_+, (4p_+^3)_{3/2})_2$	6	823 910		50
28+	[Se]	$4p^34d$	$(4p_+, 4d_-)_1$	7	866 050		80
28+	[Se]	$4p^34d$	$(4p_+, 4d_-)_3$	10	913 110		70
28+	[Se]	$4p^34d$	$(4p_+, 4d_+)_4$	12	964 703	+y	FAC
28+	[Se]	$4p^34d$	$(4p_+, 4d_+)_2$	13	1 002 100		80
28+	[Se]	$4p^34d$	$(4p_+, 4d_+)_3$	14	1 036 250		70
28+	[Se]	$4p^34d$	$(4p_+, 4d_+)_1$	15	1 071 900	+x	130
28+	[Se]	$4p^34d$	$((4p_-, (4p_+^2)_2)_{5/2}, 4d_-)_2$	29	1 285 350		120
28+	[Se]	$4p^34d$	$((4p_-, (4p_+^2)_2)_{3/2}, 4d_-)_3$	32	1 297 190		130
28+	[Se]	$4s4p^44d$	$((4s_+, (4p_+^2)_0)_{1/2}, 4d_+)_3$	65	1 922 620	+y	70
27+	[Br]	$4p^5$	$(4p_+^3)_{3/2}$	1	0		0
27+	[Br]	$4p^44d$	$((4p_+^2)_2, 4d_+)_{1/2}$	11	1 010 100		70
27+	[Br]	$4p^44d$	$((4p_+^2)_0, 4d_+)_{5/2}$	12	1 019 100		100
27+	[Br]	$4s$	$4s_+$	13	1 036 490		70
27+	[Br]	$4p^44d$	$((4p_+^2)_2, 4d_+)_{5/2}$	14	1 049 090		80

27+ [Br]	$4p^4 4d$	$((4p_-, (4p_+^3)_{3/2})_2, 4d_-)_{1/2}$	25	1 293 300	200
27+ [Br]	$4p^4 4d$	$((4p_-, (4p_+^3)_{3/2})_2, 4d_-)_{5/2}$	27	1 311 620	120
26+ [Kr]	$4p^6$	$(4p_+^4)_0$	1	0	0
26+ [Kr]	$4p^5 4d$	$((4p_+^3)_{3/2}, 4d_-)_1$	3	887 360	70
26+ [Kr]	$4p^5 4d$	$((4p_+^3)_{3/2}, 4d_+)_1$	9	1 060 100	80
26+ [Kr]	$4p^5 4d$	$(4p_-, 4d_-)_1$	13	1 317 500	120

Table 4: Energy levels of highly charged erbium. RMBPT -relativistic many-body perturbation theory [35], FAC -flexible atomic code [34], †-weighted average from two transitions

Stage and sequence	Configuration	State	Level number (FAC)	Energy (cm ⁻¹)		Unc. (cm ⁻¹)
40+ [Ni]	3d ¹⁰	(3d ₊ ⁶) ₀	1	0		0
40+ [Ni]	3d ⁹ 4s	((3d ₊ ⁵) _{5/2} , 4s ₊) ₃	2	9 931 473	+x	RMBPT
40+ [Ni]	3d ⁹ 4s	((3d ₊ ⁵) _{5/2} , 4s ₊) ₂	3	9 944 260	+x	60†
40+ [Ni]	3d ⁹ 4s	((3d ₋ ³) _{3/2} , 4s ₊) ₂	5	10 294 420	+y	RMBPT
40+ [Ni]	3d ⁹ 4p	((3d ₊ ⁵) _{5/2} , 4p ₋) ₂	6	10 596 630	+x	60
40+ [Ni]	3d ⁹ 4p	((3d ₊ ⁵) _{5/2} , 4p ₋) ₃	7	10 604 920	+x	70
40+ [Ni]	3d ⁹ 4p	((3d ₋ ³) _{3/2} , 4p ₋) ₂	8	10 951 450	+y	50
40+ [Ni]	3d ⁹ 4p	((3d ₊ ⁵) _{5/2} , 4p ₊) ₄	10	11 127 857	+z	FAC
40+ [Ni]	3d ⁹ 4d	((3d ₊ ⁵) _{5/2} , 4d ₊) ₅	23	12 275 710	+z	160
39+ [Cu]	4s	4s ₊	1	0		0
39+ [Cu]	4p	4p ₋	2	671 970		60
39+ [Cu]	4p	4p ₊	3	1 193 370		170
39+ [Cu]	4d	4d ₋	4	2 249 480		360
39+ [Cu]	4d	4d ₊	5	2 359 780		230
38+ [Zn]	4s ²	(4s ₊ ²) ₀	1	0		0
38+ [Zn]	4s4p	(4s ₊ , 4p ₋) ₁	3	638 980		50
38+ [Zn]	4s4p	(4s ₊ , 4p ₊) ₁	5	1 229 820		180
38+ [Zn]	4s4d	(4s ₊ , 4d ₋) ₂	10	2 233 040		310
38+ [Zn]	4s4d	4s ₊ , 4d ₊) ₂	14	2 453 320		370
37+ [Ga]	4p	4p ₋	1	0		0
37+ [Ga]	4p	4p ₊	2	502 760		140†

37+ [Ga]	$4s4p^2$	$4s_+$	3	659 610		50
37+ [Ga]	$4s4p^2$	$((4s_+, 4p_-)_0, 4p_+)_{3/2}$	4	1 074 090		140
37+ [Ga]	$4s4p^2$	$((4s_+, 4p_-)_1, 4p_+)_{5/2}$	5	1 131 460		240
37+ [Ga]	$4s4p^2$	$((4s_+, 4p_-)_1, 4p_+)_{3/2}$	6	1 216 140		170
37+ [Ga]	$4s4p^2$	$((4s_+, 4p_-)_1, 4p_+)_{1/2}$	7	1 237 970		220
37+ [Ga]	$4d$	$4d_-$	9	1 619 300		320
36+ [Ge]	$4p^2$	$(4p_-^2)_0$	1	0		0
36+ [Ge]	$4p^2$	$(4p_-, 4p_+)_2$	3	488 190		190
36+ [Ge]	$4s4p^3$	$(4s_+, 4p_+)_{1/2}$	7	1 216 340		180
36+ [Ge]	$4p4d$	$(4p_-, 4d_-)_1$	11	1 638 250		330
35+ [As]	$4p^3$	$(4p_+^3)_{3/2}$	1	0		0
35+ [As]	$4p^3$	$(4p_-, (4p_+^2)_2)_{3/2}$	2	440 827	+x	FAC
35+ [As]	$4p^3$	$(4p_-, (4p_+^2)_2)_{5/2}$	3	479 420	+x	70
35+ [As]	$4p^24d$	$4d_-$	6	1 061 840	+x	90
35+ [As]	$4s4p^4$	$(4s_+, (4p_+^2)_2)_{5/2}$	7	1 089 300	+x	50
35+ [As]	$4p^24d$	$((4p_-, 4p_+)_{1/2}, 4d_+)_{7/2}$	17	1 610 740	+x	170
35+ [As]	$4p^24d$	$((4p_-, 4p_+)_{1/2}, 4d_-)_{5/2}$	20	1 646 720		310
35+ [As]	$4p^24d$	$((4p_-, 4p_+)_{1/2}, 4d_-)_{3/2}$	21	1 652 980		370
34+ [Se]	$4p^4$	$(4p_+^4)_2$	1	0		0
34+ [Se]	$4p^4$	$(4p_+^2)_0$	2	63 215	+x	FAC
34+ [Se]	$4p^34d$	$(4p_+, 4d_-)_3$	9	1 089 480		180
34+ [Se]	$4p^34d$	$(4p_+, 4d_+)_{1/2}$	13	1 249 340		180
34+ [Se]	$4p^34d$	$(4p_+, 4d_+)_{3/2}$	14	1 266 900		190
34+ [Se]	$4p^34d$	$(4p_+, 4d_+)_{1/2}$	15	1 320 360	+x	190
34+ [Se]	$4p^34d$	$((4p_-, (4p_+^2)_2)_{5/2}, 4d_-)_2$	29	1 660 300		590
34+ [Se]	$4p^34d$	$((4p_-, (4p_+^2)_2)_{3/2})_3$	30	1 668 630		490

33+	[Br]	$4p^5$	$(4p_+^3)_{3/2}$	1	0	0
33+	[Br]	$4p^4 4d$	$((4p_+^2)_2, 4d_-)_{3/2}$	3	1 043 590	130
33+	[Br]	$4p^4 4d$	$((4p_+^2)_2, 4d_-)_{5/2}$	5	1 056 800	530
33+	[Br]	$4p^4 4d$	$((4p_+^2)_2, 4d_-)_{7/2}$	6	1 077 240	160
33+	[Br]	$4p^4 4d$	$((4p_+^2)_2, 4d_+)_{3/2}$	12	1 270 380	210
33+	[Br]	$4s$	$4s_+$	13	1 272 610	160
33+	[Br]	$4p^4 4d$	$((4p_+^2)_2, 4d_+)_{5/2}$	14	1 288 160	190
33+	[Br]	$4p^4 4d$	$((4p_-, (4p_+^3)_{3/2})_2, 4d_-)_{1/2}$	24	1 672 540	190
33+	[Br]	$4p^4 4d$	$((4p_-, (4p_+^3)_{3/2})_2, 4d_-)_{3/2}$	25	1 672 540	190
33+	[Br]	$4p^4 4d$	$((4p_-, (4p_+^3)_{3/2})_2, 4d_-)_{5/2}$	26	1 681 280	170
32+	[Kr]	$4p^6$	$(4p_+^4)_0$	1	0	0
32+	[Kr]	$4p^5 4d$	$((4p_+^3)_{3/2}, 4d_-)_1$	3	1 062 370	130
32+	[Kr]	$4p^5 4d$	$((4p_+^3)_{3/2}, 4d_+)_1$	9	1 303 010	200
32+	[Kr]	$4p^5 4d$	$(4p_-, 4d_-)_1$	13	1 684 740	380
31+	[Rb]	$4d$	$4d_-$	1	0	0
31+	[Rb]	$4d$	$4d_+$	2	95 819	+x FAC
31+	[Rb]	$4p^5 4d^2$	$((4p_+^3)_{3/2}, (4d_-^2)_2)_{5/2}$	5	1 067 570	150
31+	[Rb]	$4p^5 4d^2$	$((4p_+^3)_{3/2}, (4d_-^2)_2)_{7/2}$	6	1 082 580	+x 120
31+	[Rb]	$4p^5 4d^2$	$((4p_+^3)_{3/2}, (4d_+^0)_2)_{3/2}$	8	1 124 800	170
31+	[Rb]	$4p^5 4d^2$	$((4p_+^3)_{3/2}, 4d_-)_1, 4d_+)_{3/2}$	11	1 158 890	160
31+	[Rb]	$4p^5 4d^2$	$((4p_+^3)_{3/2}, 4d_-)_3, 4d_+)_{7/2}$	14	1 179 840	+x 140
31+	[Rb]	$4p^5 4d^2$	$((4p_+^3)_{3/2}, 4d_-)_2, 4d_+)_{7/2}$	16	1 207 390	+x 150
31+	[Rb]	$4p^5 4d^2$	$((4p_+^3)_{3/2}, 4d_-)_3, 4d_+)_{5/2}$	17	1 211 910	180
31+	[Rb]	$4p^5 4d^2$	$((4p_+^3)_{3/2}, (4d_+^2)_4)_{5/2}$	21	1 255 770	200
31+	[Rb]	$4p^5 4d^2$	$((4p_+^3)_{3/2}, (4d_+^2)_4)_{5/2}$	22	1 255 770	200
31+	[Rb]	$4p^5 4d^2$	$((4p_+^3)_{3/2}, 4d_-)_3, 4d_+)_{3/2}$	25	1 279 690	190
31+	[Rb]	$4p^5 4d^2$	$((4p_+^3)_{3/2}, 4d_-)_3, 4d_+)_{1/2}$	28	1 341 500	210
31+	[Rb]	$4f$	$4f_-$	32	1 446 140	240

31+ [Rb]	$4p^5 4d^2$	$(4p_-, (4d_-^2)_2)_{5/2}$	34	1 589 690	300
31+ [Rb]	$4p^5 4d^2$	$(4p_-, (4d_-^2)_0)_{1/2}$	40	1 674 780	510
31+ [Rb]	$4p^5 4d^2$	$(4p_-, (4d_+^2)_2)_{5/2}$	45	1 720 010	400